

SUPPLEMENT TO STATE OF THE CALIFORNIA CURRENT 2012–13: NO SUCH THING AS AN “AVERAGE” YEAR

NORTH PACIFIC CLIMATE INDICES

Data and Analysis The Pacific Decadal Oscillation (PDO) values were obtained online where there is also a description of the methodology and interpretation: <http://jisao.washington.edu/pdo/PDO.latest>.

Multivariate ENSO Index (MEI) values and interpretation were obtained from <http://www.esrl.noaa.gov/psd/enso/mei/>.

North Pacific Gyre Oscillation (NPGO) values and interpretations were obtained from <http://www.o3d.org/npgo/>.

NORTH PACIFIC CLIMATE PATTERNS

Data and Analysis Monthly data for winds and SST in Figure S1 obtained from the NOAA–CIRES Climate Diagnostics.

Upwelling values (CUI; fig. 3 and fig. S2) and interpretations were obtained from http://www.pfeg.noaa.gov/products/las/docs/global_upwell.html.

December sea level height data (fig. 4) and interpretation were obtained from <http://ilikai.soest.hawaii.edu/>.

Supplemental Results SST anomalies were predominantly negative over the western Pacific in summer, in

support of the PDO values and in contrast to the MEI signals. Concomitant with a rise in the PDO to climatological mean values in 2013 is an increase in SST anomalies in April 2013 over much of the central Pacific, though SST anomalies remain negative along the near-shore California coast (fig. S1).

HF Radar Surface Current Observations

Data and Analysis These data on surface currents were obtained from high frequency (HF) Radar, with vectors calculated hourly at 6-km resolution using optimal interpolation (Kim et al. 2008; Terrill et al. 2006). Data are averaged to 20-km resolution prior to display. Real-time displays can be viewed at www.sccoos.org/data/hfrnet/ and www.cencoos.org/sections/conditions/Google_currents/ as well as at Web sites maintained by the institutions that contributed data reported here (listed in Acknowledgments).

Supplemental Results In spring 2012 (March–May), a strong offshore jet was evident off Cape Mendocino Bight (40.5°N) and extending offshore south of Point Arena (39°N)(fig. S4). Similar weak features are seen south of Newport OR, Cape Blanco, Point Año Nuevo,

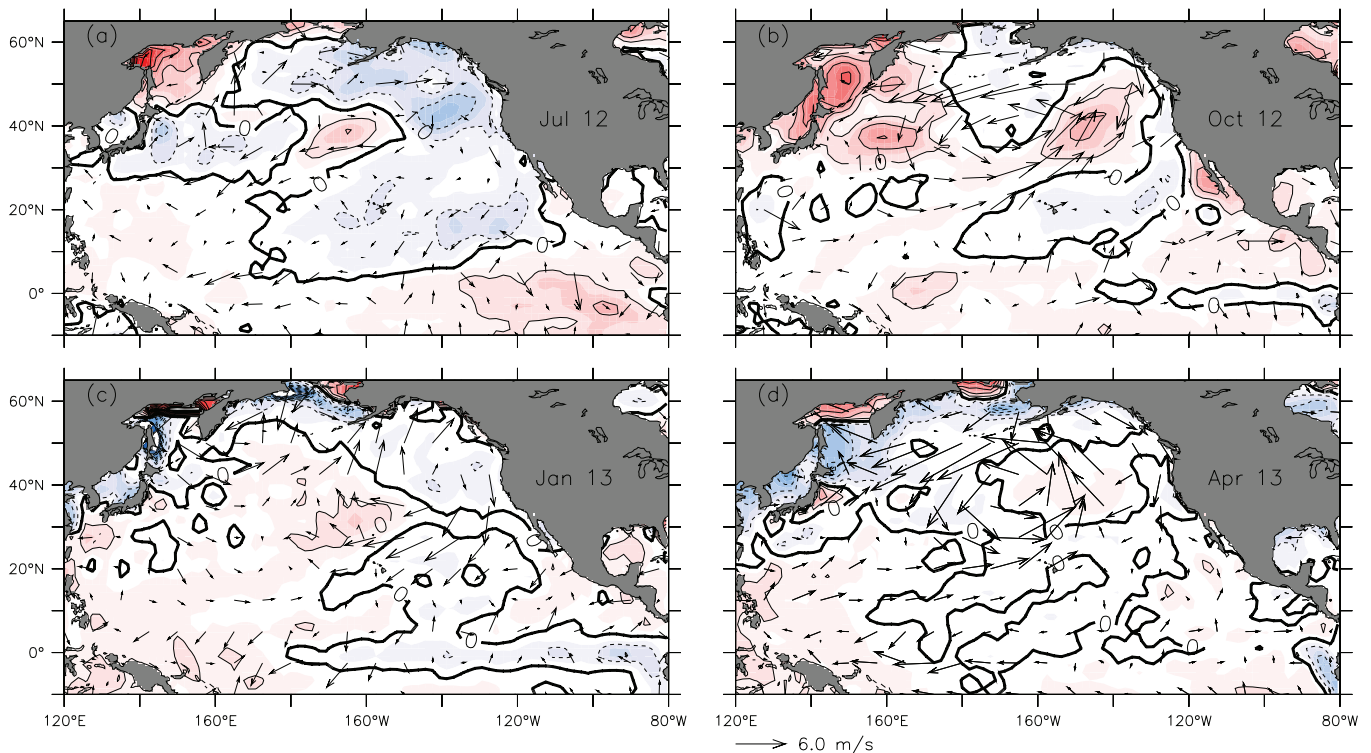


Figure S1. Anomalies of surface wind velocity and sea surface temperature (SST) in the North Pacific Ocean, July 2012, October 2012, January 2013, and April 2013. Arrows denote magnitude and direction of wind anomaly (scale arrow at bottom). Contours demote SST anomaly. Shading interval is 0.5°C and contour interval is 1.0°C. Negative (cool) SST anomalies are shaded blue. Wind climatology period is 1968–96. SST climatology period is 1950–79.

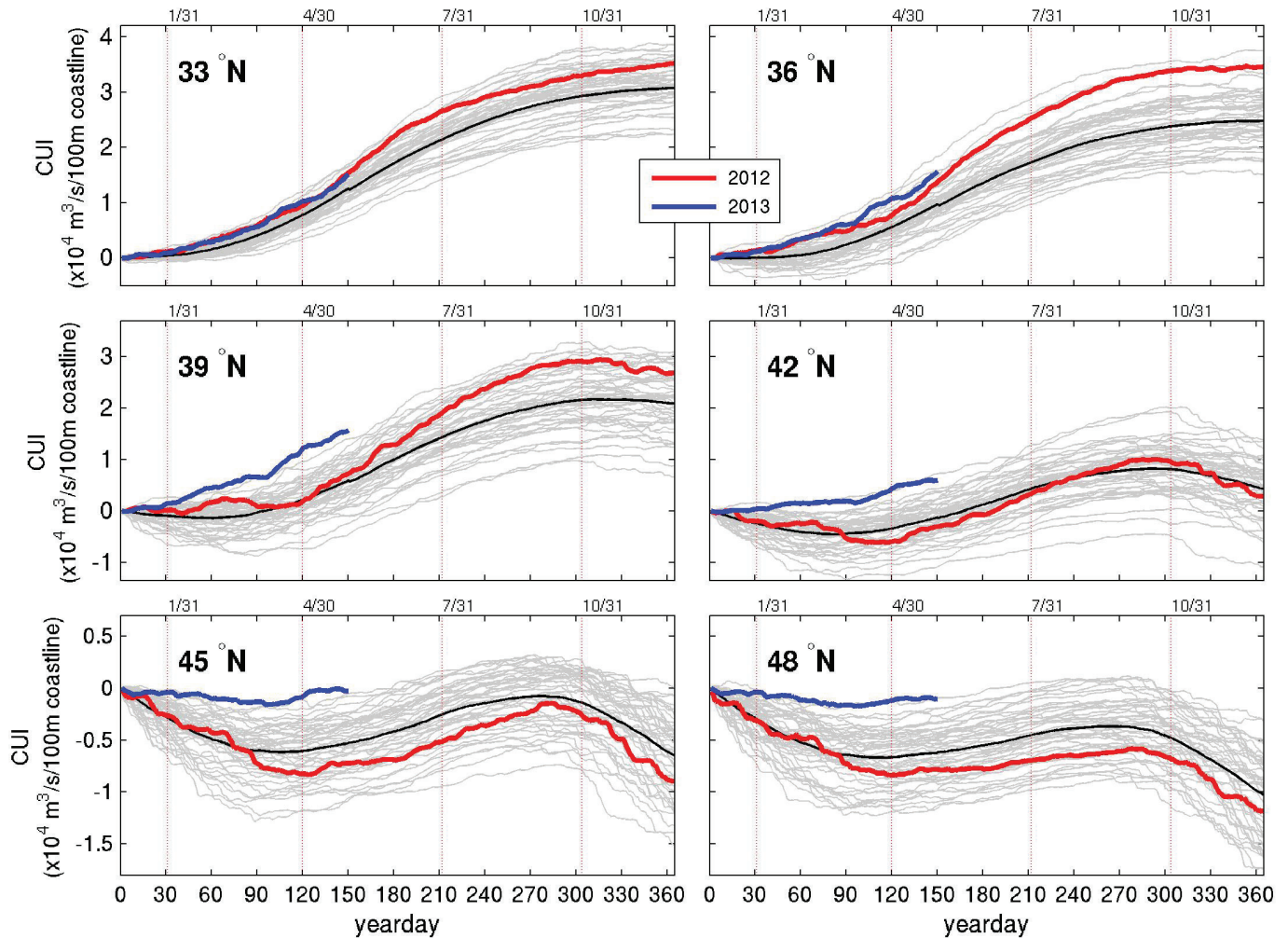


Figure S2. Cumulative upwelling from January 1 calculated from Bakun Index at indicated locations along the West Coast of North America for 1967–2011 (grey lines), the mean value for the period 1967–2011 (black line), 2012 (red line), and 2013 (blue line).

and Point Conception—but northward flows were evident off Washington and a squirt-like offshore flow is seen immediately north of Cape Mendocino, which strengthens through summer and appears to persist even into fall. During summer, the surface flow is stronger and directed more offshore.

The cape-associated jets also strengthened—notably the eddy-like feature between 37° and 40°N (reminiscent of the 2009 occurrence of the Mendocino Eddy noted in Bjorkstedt et al. 2010) and a jet appears south of Point Sur (36.5°N). Inshore of Cape Mendocino– Point Arena feature, a strong coastal jet is seen immediately south of Point Arena; illustrating the dual influences of local wind forcing (Arena shelf jet) and large-scale flow features (Mendocino Eddy). In summer, flow is southward everywhere other than in the Southern California Bight (32°–34°N). Westward flow out of the Santa Barbara Channel appears to enhance offshore flow west of Point Conception (34.5°N). During fall, there is a

general weakening of surface currents and an unusual tendency for northward flow throughout the region, except in the region south of Point Arena (37–39°N). This southward flow off Point Arena persists through the winter, extending again as far north as Cape Mendocino, and results in exceptionally strong southward flows off Point Arena during upwelling conditions in May–June 2013 (processed data not available; speeds up to 80 cm/s). The unusual offshore flows in this region during winter extend throughout central California, as far as the more usual offshore flow at Point Conception. In winter, northward flow is only seen to the north of Cape Blanco, strongest off the mouth of the Columbia River.

Coast-wide Analysis of Chlorophyll

Data and Analysis Chlorophyll *a* values were obtained from the coastwatch web page (<http://coastwatch.pfeg.noaa.gov/erddap>). Monthly composites of Aqua MODIS science quality chlorophyll *a* values were

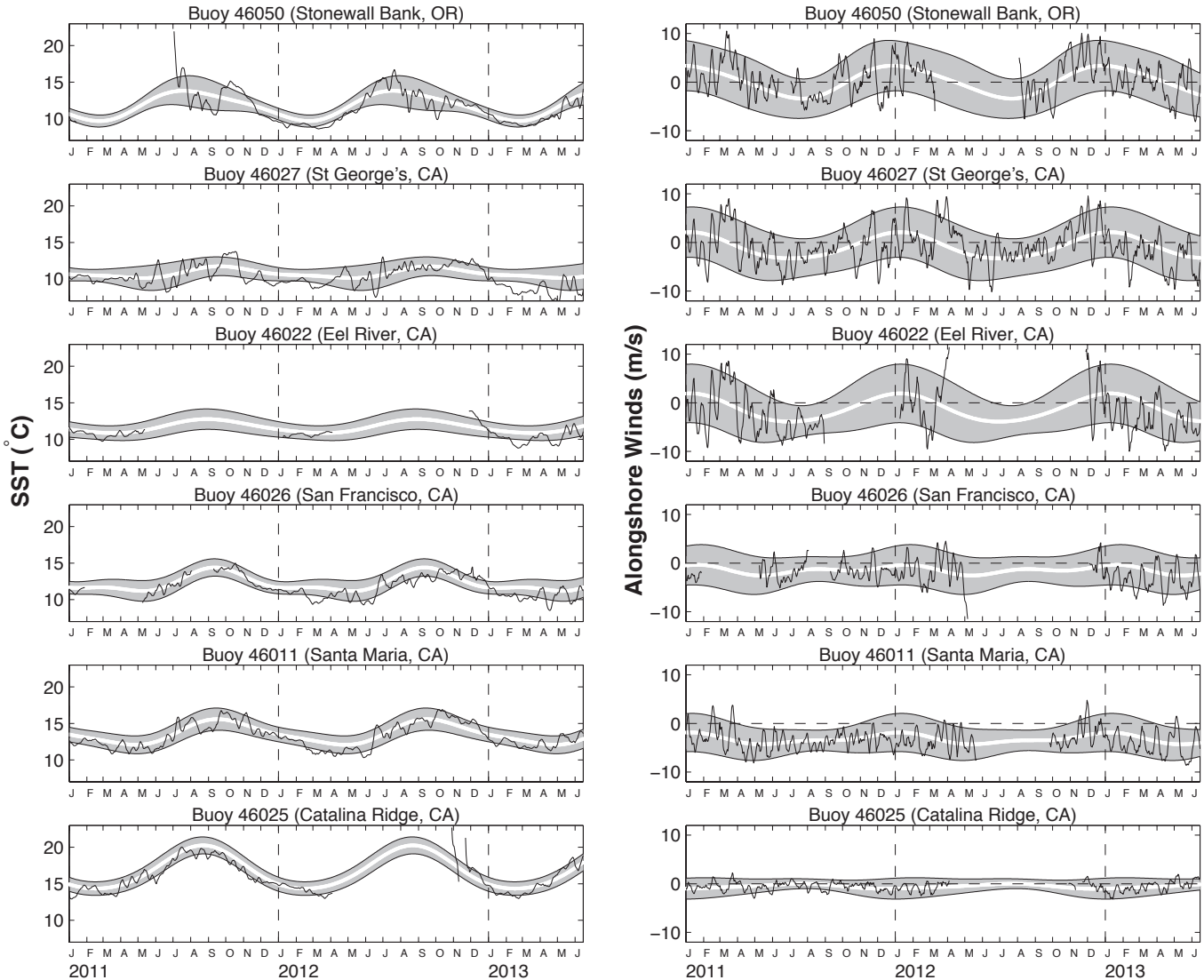


Figure S3. Time series of daily sea surface temperatures (left) and alongshore winds (right) from various National Data Buoy Center (NDBC) coastal buoys along the CCS for January 2011 to June 2013. The wide white line is the biharmonic annual climatological cycle at each buoy. Shaded areas are the standard errors for each Julian day. Series have been smoothed with a 7-day running mean. Data provided by NOAA NDBC. Coordinates for buoy locations are at <http://www.ndbc.noaa.gov/>.

used to calculate the spring anomalies. The anomalies were calculated by subtracting a spring average (March–May) from a spring climatology based on the period from 2003 to 2013.

REGIONAL SUMMARIES OF HYDROGRAPHIC AND PLANKTONIC DATA

Northern California Current: Newport Hydrographic Line

Data and Analysis Regular sampling of the Newport Hydrographic Line continued on a biweekly basis along the inner portions of the line (out to 25 nm). Details on sampling protocols are available in previous reports and at <http://www.nwfsc.noaa.gov/research/divisions/fed/oep/ka-hydrography-zoo->

[ichthyoplankton.cfm](http://www.nwfsc.noaa.gov/research/divisions/fed/oep/ka-hydrography-zoo-ichthyoplankton.cfm). Temperature anomalies along the Newport line are based on the Smith et al. (Smith et al. 2001) climatology. Copepod data are based on samples collected with a 0.5 m diameter ring net of 202 μm mesh, hauled from near the bottom to the sea surface. A TSK flow meter was used to estimate distance towed.

Northern California Current: Trinidad Head

Data and Analysis See <http://swfsc.noaa.gov/HSU-CFORT/> for description of methods. Surveys are carried out on Humboldt State University's R/V *Coral Sea*.

Central California

Data and Analysis Data on temperature and salinity at the surface and 100 m for Monterey Bay are based on MBARI monthly cruises and mooring data.

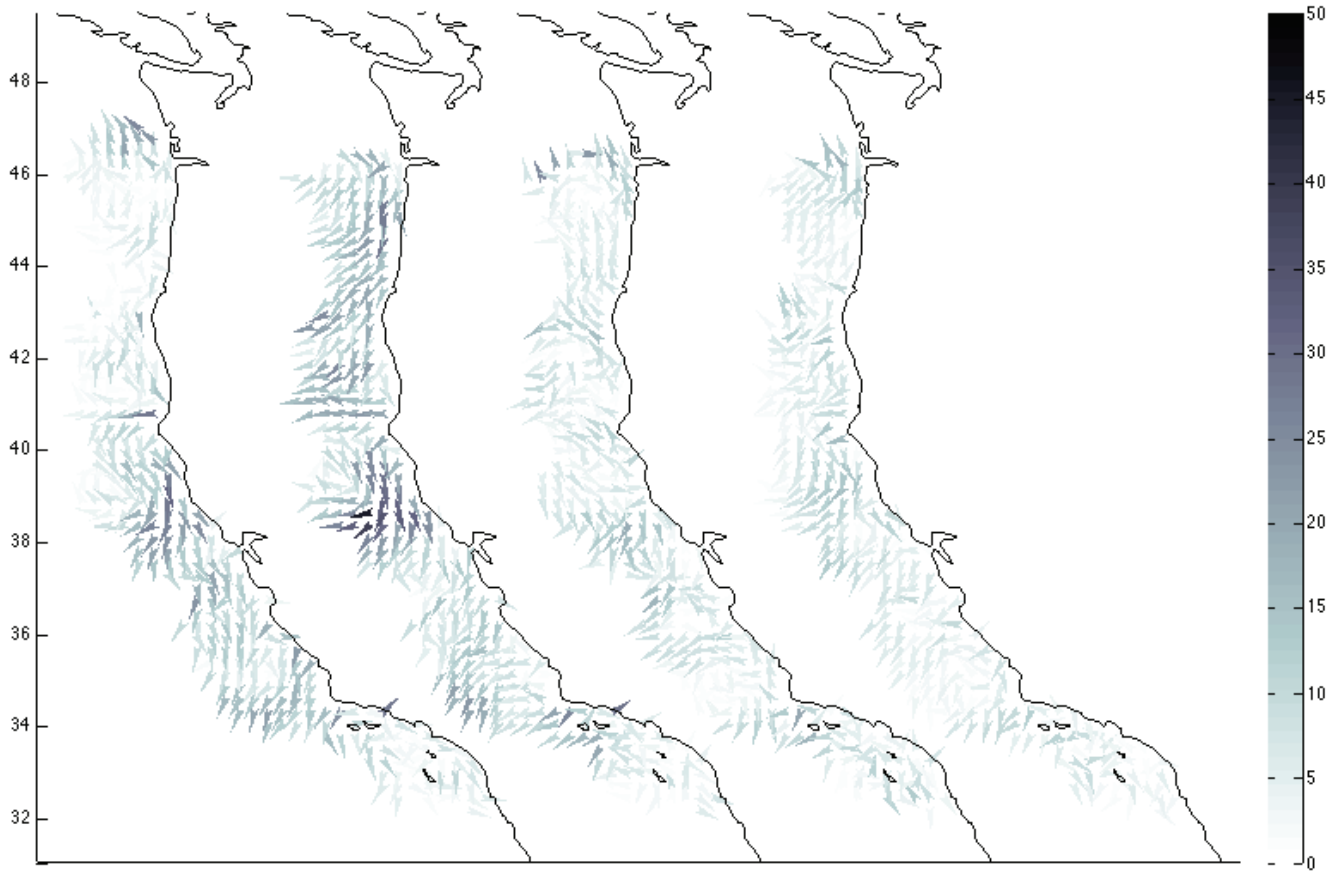


Figure S4. Mean maps of high frequency (HF) radar surface currents observed quarterly throughout the CCS. From left to right, the panels present data from left to right for spring (March–May, 2012), summer (June–August, 2012), fall (September–November, 2012), and winter (December–February, 2013). Current speed is indicated by shading and direction given by orientation of arrow extending from observation location. For clarity, currents are displayed with spatial resolution of 30 km.

HF radar data on surface current vectors were calculated hourly at 2-km resolution using standard CODAR software (real-time displays can be viewed at www.bml.ucdavis.edu/boon/current_plots.html). Plotted data are averaged over spatial bins west of Point Reyes: “near-shore” 38°00–10′N and 123°00–10′W; “offshore” 38°00–10′N and 123°20–40′W). Upwelling index values are from www.pfeg.noaa.gov and sea level data are from tidesandcurrents.noaa.gov.

Supplemental Results A time-series of surface flow past Point Reyes (38°N) illustrates variability in the timing, strength, and duration of southward flows over the past 12 years (fig. S5). In 2012, the Point Arena coastal jet (fig. S5) appears as strong southward flow past Point Reyes, starting suddenly in March or April and weakening already in June. Although significant southward flow persists offshore through summer and fall, mean flows nearshore are close to zero after June (and mean sea level rises). This flow seasonality is in contrast to the upwelling index, which typically peaks in June and remains strong through July. However recent work by Garcia-Reyes and Largier 2012 show that observed

winds follow a different seasonal cycle, peaking in early summer, more consistent with alongshore currents. In some years, strong southward flow persists offshore through late summer (2004, 2007, 2009), presumably due to offshore forcing associated with the presence of an anticyclonic mesoscale eddy south of Point Arena (Kaplan et al. 2009; Largier et al. 1993)—this situation appears to be developing also in 2013. The seasonality of flow past Point Reyes is somewhat normal in 2012, but southward flows were a bit weaker than usual and the upwelling index peak was a bit stronger than usual. During winter, a weak and uniform northward mean flow was observed, which is quite typical. As in previous years, nearshore flow past Point Reyes correlates closely with mean sea level. During 2012 and 2013, alongshore flows past Point Reyes exhibited weak anomalies (<5 cm/s for all months).

Southern California

Data and Analysis Results are presented as time series of averages over all 66 stations covered during a cruise or as anomalies of such values. The mixed layer

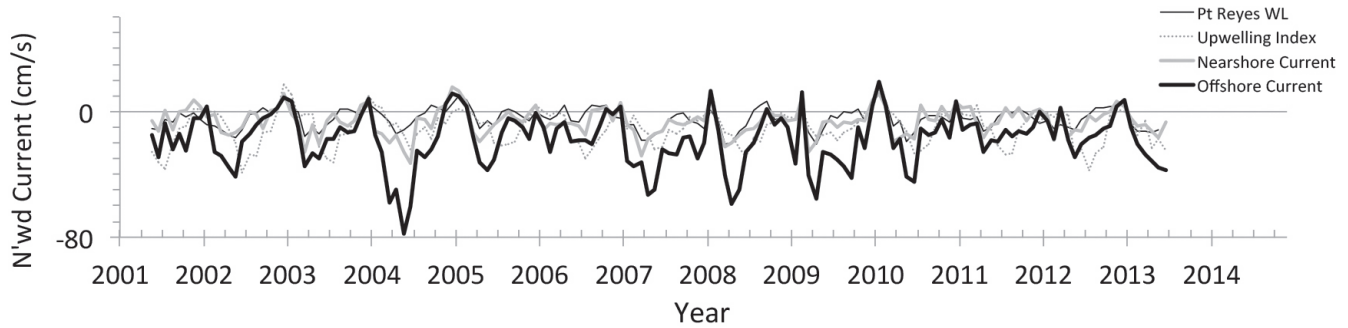


Figure S5. Monthly averages of spatially averaged surface flow past Point Reyes California between 30 and 60 km offshore (offshore current; thick black line) and between 0 and 15 km offshore (nearshore current; thick grey line). Positive values indicate northward flow in cm/s. Also shown is monthly average cross-shelf Ekman transport indexed as the negative Upwelling Index at 39°N (fine grey dashed line; positive values indicate onshore Ekman transport in units of 10 m³/s per 100 m of coastline) and monthly average sea level at Point Reyes relative to 1 m above MLLW (fine black line; units cm).

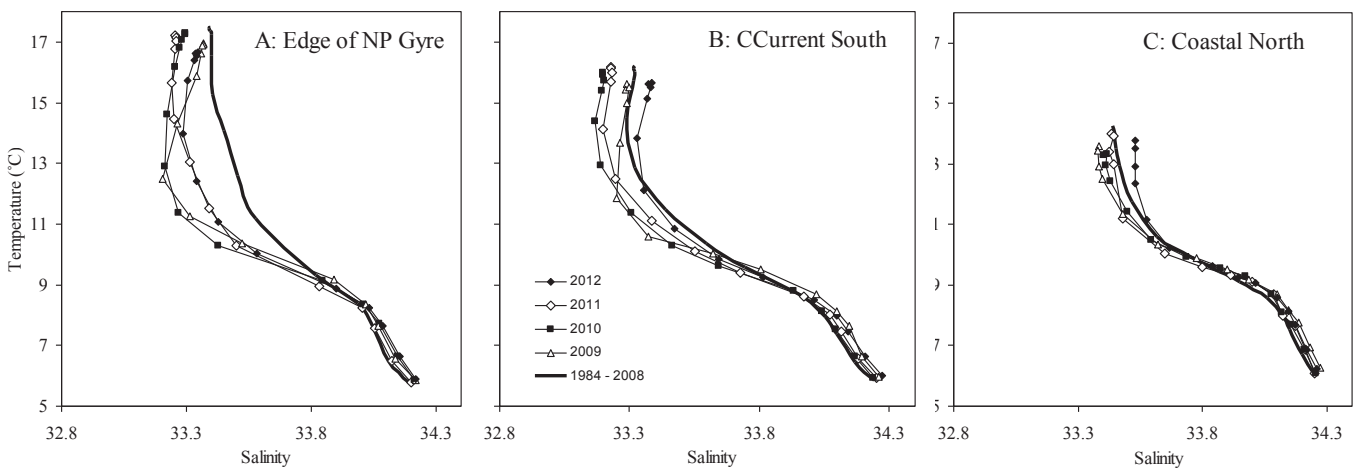


Figure S6. Temperature-salinity (TS) plots for three representative areas of the CalCOFI region. A. The edge of the central gyre (Lines 90–93, Stations 100–120), B. the southern California Current region (Lines 87–93, Stations 60–90) and C. the coastal areas in the north (Lines 77–80, Stations 60 and inshore). Each data point represents the average TS characteristic of one standard depth level for the specified time periods, i.e., 1984 to 2008, 2009, 2010, 2011, and 2012.

depth is calculated using a density criterion and is set either to 12 m or to the halfway point between the two sampling depths where the sigma-theta gradient first reaches values larger than 0.002 per m, whichever is larger. The nitracline depth is defined as the depth where concentrations of nitrate reach values of 1 μm , calculated from measurements at discrete depths using linear interpolation. Mesozooplankton displacement volumes for individual stations were log-transformed and then averaged over all stations. Zooplankton displacement volumes are determined for whole samples (total) and for samples from which specimens are removed that have a displacement volume larger than 5 ml (small fraction). Statistical analyses were carried out using the Statistics or System Identification toolboxes of Matlab (Version 7.12, The MathWorks Inc., Natick, MA, 2012).

Baja California

Data and Analysis Quarterly surveys were conducted on the Mexican R/V *Francisco de Ulloa*, a seabird

CTD instrument was used in the IMECOCAL surveys off Baja California. Temperature and conductivity sensors were factory calibrated prior to each survey. Data processing was carried out following Garcia-Cordova et al. 2005. The vertical resolution for each profile was 1 dbar. A total of 54 quarterly surveys were used in the present study, which were performed from October 1997 to February 2013. To obtain the time series of the upper layer temperature and salinity anomalies, the overall mean for the period 1997–2013 was first calculated; after that, anomalies were computed by contrasting measured values at each location; and finally the annual harmonic was extracted from the anomalies.

Phytoplankton chlorophyll data were analyzed from samples collected from 1998–2013 surveys. The instruments used included a CTD/Rosette casts to 1000 m (depth permitting) and discrete water samples to determine chlorophyll *a* from the upper 200 m collected with 5-liter Niskin bottles. Water column chlorophyll was measured from 1-liter samples, filtered onto What-

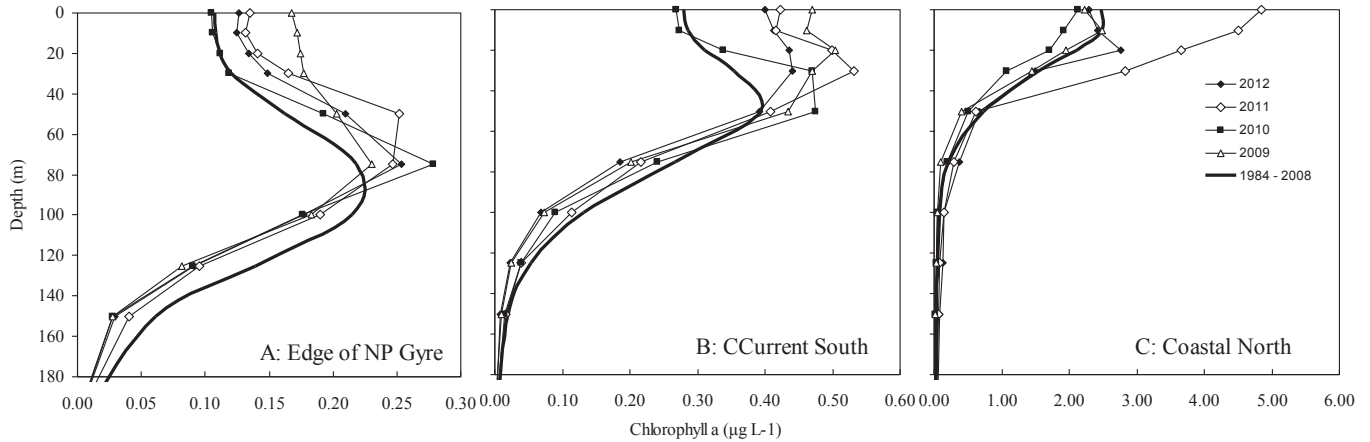


Figure S7. Depth profiles of chlorophyll *a* for the three areas of the CalCOFI region: (A) the edge of the central gyre, (B) the southern California Current region, and (C) the northern coastal areas.

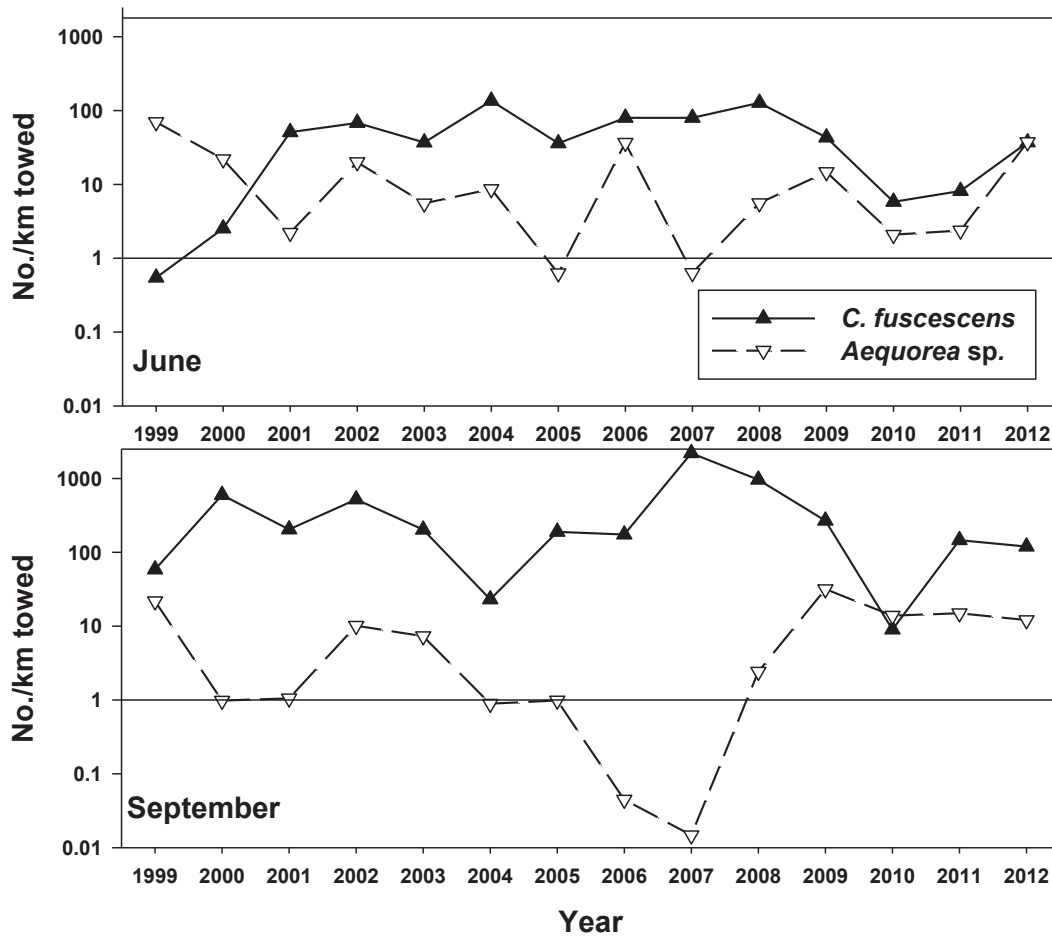


Figure S8. Catches of the three dominant species of jellyfish in pelagic surveys off the coast of Oregon and Washington in June and September.

man GF/F filters, following the fluorometric method (Garcia-Cordova et al. 2005; Holm-Hansen et al. 1965; Yentsch and Menzel 1963) with adaptations of Venrick and Hayward (1984). 10-m chlorophyll *a* anomalies were calculated for the period 1998–2013 (February), after remove the long-term mean of the data. Zooplankton

was sampled with bongo net tows from 200 m to the surface. Nighttime samples were selected to count copepods and euphausiids (1998–2013). For more reference about water samples collections and zooplankton techniques visit the IMECOCAL web page: <http://imecocal.cicese.mx>

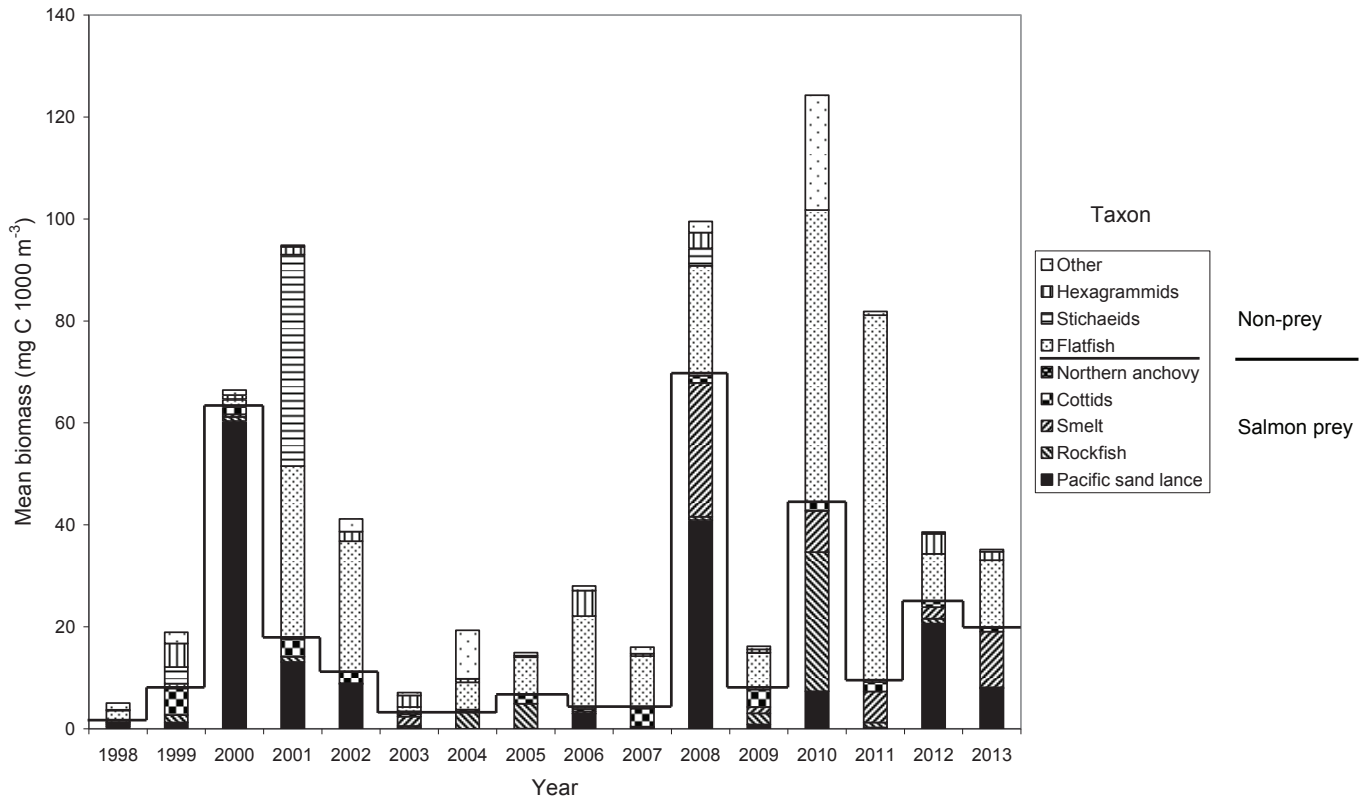


Figure S9. Annual mean biomass (mg C 1000 m⁻³) of the five important salmon prey taxa (below solid line) and four other dominant larval fish taxa (above solid line) collected during winter (January–March) in 1998–2013 along the Newport Hydrographic line off the coast of Oregon (44.65°N, 124.18–124.65°W). Figure expanded from one presented in Daly et al. 2013.

GELATINOUS ZOOPLANKTON

Northern California

Data and Analysis Salps (mostly *Thetys vagina* and *Salpa fusiformis*) have been enumerated from large fine-mesh midwater trawl collections off Oregon and Washington since 2004. Data come from four-cross shelf transects typically sampled from May through September (Phillips et al. 2009).

SYNTHESIS OF OBSERVATIONS ON HIGHER TROPHIC LEVELS

Pelagic Fishes off Northern California Current System

Data and Analysis Survey protocols for NWFSC–NOAA Bonneville Power Authority are available at <http://www.nwfsc.noaa.gov/research/divisions/fed/oeip/kp-juvenile-salmon-sampling.cfm>.

See Auth 2011 and Phillips et al. 2009 for the complete May and July larval and juvenile sampling methods, respectively, and Daly et al. 2013 for the winter larval sampling methods. Briefly, larval samples were collected primarily at night using oblique tows of a 60 cm bongo net (335 μm) from 100 m (or within 5 m of the

floor). Samples were preserved in 95% ethanol, which was replaced with new 95% ethanol after ca. 72 hours. All larval fish in each sample were removed, counted, and identified to the lowest taxonomic level possible.

Supplemental Results The biomass of ichthyoplankton in 2013 from winter collections along the Newport Hydrographic Line were above average and ranked 5th in the 16 year time series (1998–2013), predicting good food conditions for juvenile salmon during the 2013 out migration (fig. S9). Winter ocean conditions based on average PDO in October–December 2012 predicted very closely the biomass of winter ichthyoplankton larvae in January–March 2013 (predicted = 1.0 log_e C mg 1000m⁻³; actual = 1.16 log_e C mg 1000m⁻³). Additionally, the proportion of the total larvae considered important salmon prey was above average (ranked 4th out of 16 years at 48.8%; data range from a low of 7.4% in 2011, and a high of 95% in 2000). The community structure of the winter larvae ranked 9th due to the high proportion of the prey biomass that were smelt larvae, which are typical of years of moderate survival of salmon, and average biomass of Pacific sand lance and cottid larvae, which are typically prey eaten in higher salmon survival out migration years. There was a low proportion of rockfish larvae in the winter of 2013, which is a positive indi-

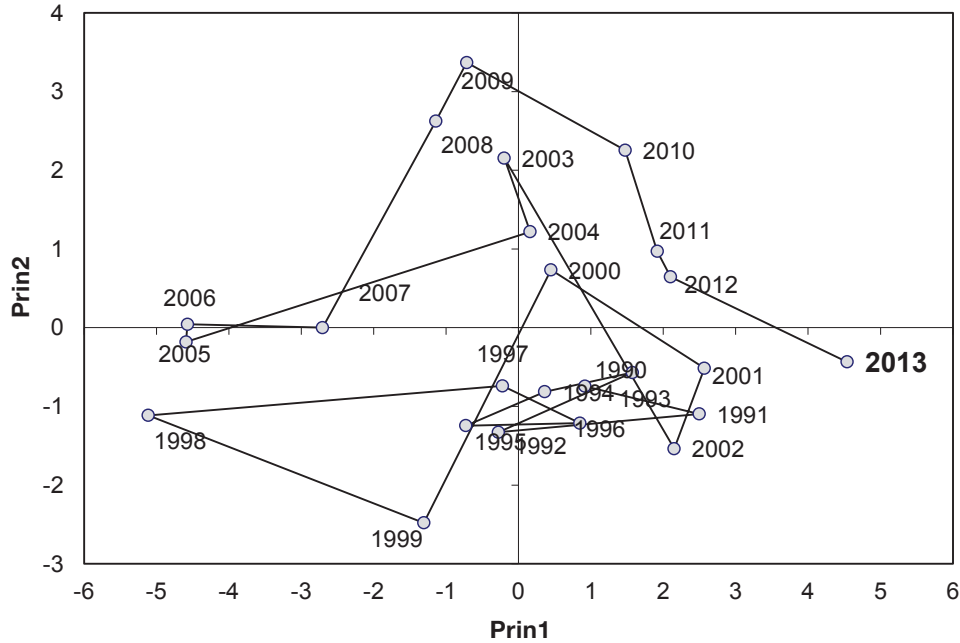


Figure S10. Principal component scores plotted in a phase graph for the fourteen most frequently encountered species groups sampled in the central California core area in the 1990–2013 period.

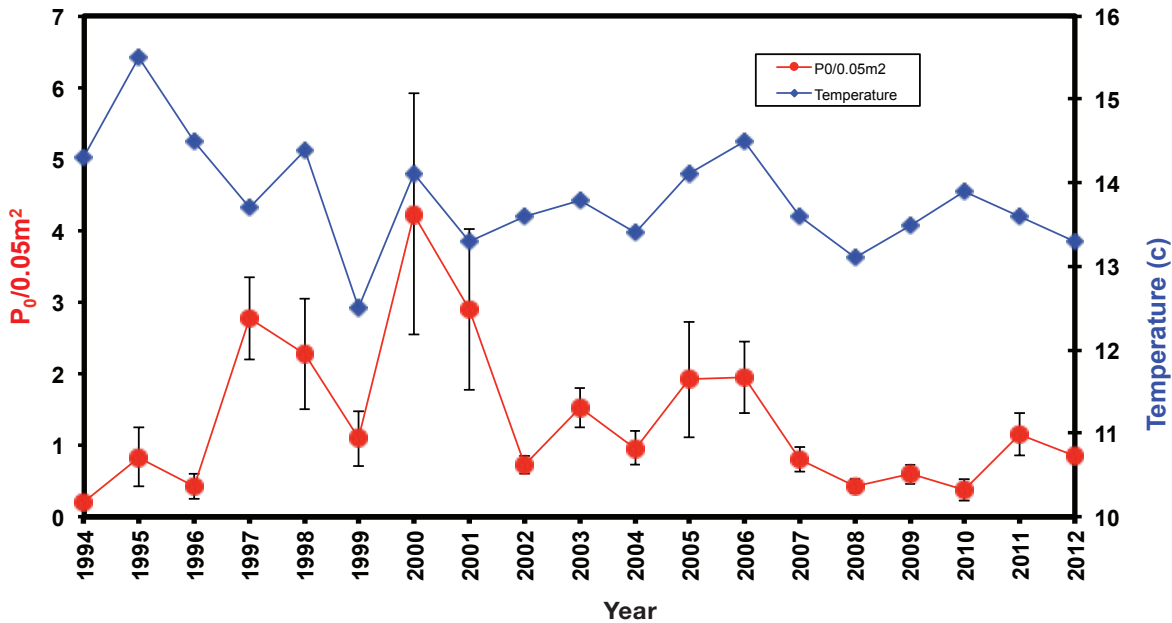


Figure S11. Time series of daily egg production ($P_o/0.05\text{ m}^2$) of Pacific sardine and average sea surface temperature during pelagic egg surveys conducted during March–April of each year.

cator for food conditions during the 2013 out migration period. Overall, winter larval biomass and community structure would predict an above average food community for juvenile salmon in 2013.

Pelagic Fishes off Central California Current System

Data and Analysis Observations reported here are based on midwater trawl surveys that target small (1–20

cm) pelagic fishes and invertebrates conducted off central California (a region running from just south of Monterey Bay to just north of Point Reyes, CA, and from near the coast to about 60 km offshore) since 1983 (see Sakuma et al. 2006 for methods and details on spatial extent of survey). Cruises have been conducted on the NOAA ship *David Starr Jordan* (1983–2008), the NOAA ship *Miller Freeman* (2009), the F/V *Frosti* (2010), the F/V *Excalibur* (2011), and the NOAA ship *Bell M.*

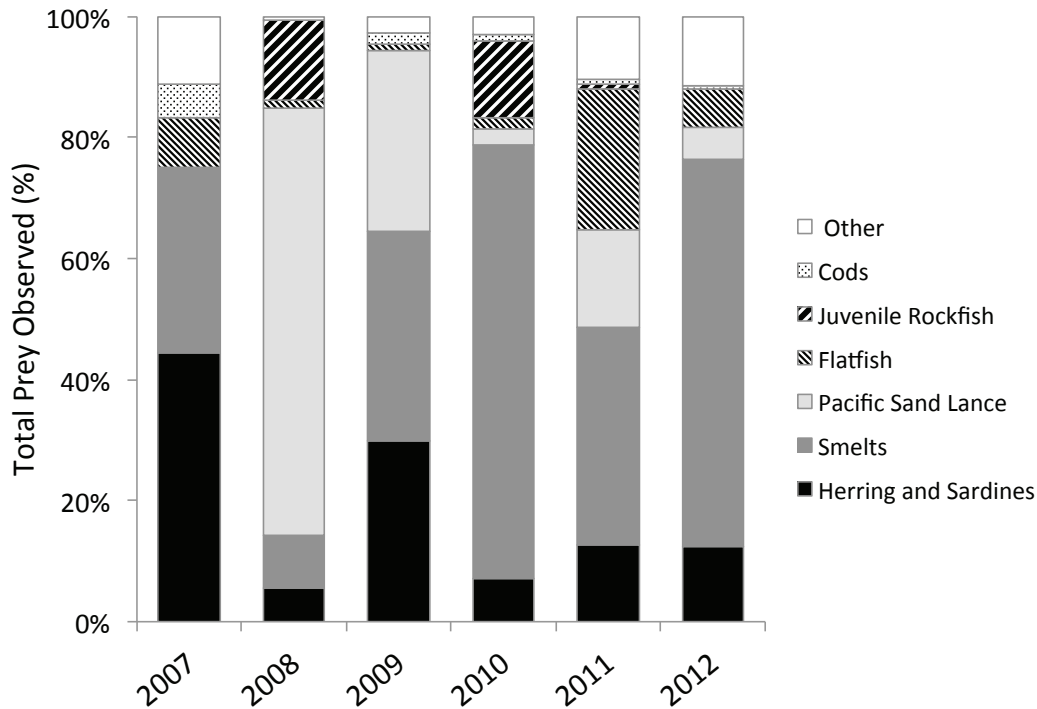


Figure S12. Composition of prey delivered to common murre chicks between 2007 and 2012 at Yaquina Head Outstanding Natural Area, Oregon.

Shimada (2012). Certain taxa were not consistently enumerated prior to 1990 (e.g., krill and market squid). Data for the 2013 survey presented here are preliminary, and data collected since 2009 do not account for potential vessel-related differences in catchability. Most taxa reported are considered to be well sampled, but the survey was not specifically designed to accurately sample krill.

Supplemental Results As with past reports (e.g., Bjorkstedt et al. 2011), the trends observed in the six indicators shown in Figure 25 are consistent with trends across a broader suite of taxa within this region, with the first and second components (of a principle components analysis of 15 of the dominant taxon) explaining approximately 36% and 16% of the variance in the data, respectively. Loadings of these groups indicate strong covariance among young-of-the-year groundfish (rockfish, sanddabs, and Pacific hake), cephalopods and euphausiids, which in turn tend to be negatively correlated over time with coastal pelagic and mesopelagic species. As with the 2011 results, 2012 continued to indicate a pelagic micronekton community structure to conditions similar to those seen in the early 1990s and early 2000s (fig. S10). However, the spatial patterns of abundance will also be the target of future analysis, as anecdotally these patterns may not have been typical of previous cool, productive periods. Specifically, as there was some suggestion that small gelatinous zooplankton were at greater levels of abundance in off-

shore waters, while more coastal waters experienced relatively greater abundance levels of krill, squid, and juvenile groundfish.

Salmon: Sub-yearling juvenile Chinook salmon (80–250 mm fork length, FL) were less abundant in the catches in 2012 than in the previous two years (fig. 26). The larger 2011 cohort of juvenile Chinook salmon was still relatively abundant as second-ocean-year fish in 2012, now as individuals 300–500 mm fork length (FL) and making up the majority of all Chinook captured in 2012. The 2010 juvenile cohort, which appeared to have very high relative overwinter survival in 2011 and was well represented (as 300–500 mm FL fish) in the July 2011 survey, was still present in June 2012 as third-ocean-year fish (>500 mm FL). This resulted in the capture of more adult Chinook salmon (>500 mm FL) in 2012 than in either of the previous two years.

Unlike Chinook salmon, the abundance of juvenile coho salmon (100–300 mm FL) was similar in the summer of 2011 and 2012 (fig. 26). Significantly more juvenile coho salmon were caught in either of those two years than in July 2010. As with Chinook, relative overwinter survival of the 2010 juvenile coho cohort appeared to be relatively high, and this group was observed as numerous two-year old fish (>500 mm FL) in July 2011. Also like Chinook, overwinter survival of the 2011 coho cohort appeared to be lower than overwinter survival of the 2010 cohort. Fewer large (>500 mm FL) coho were taken in 2012 than in 2011.

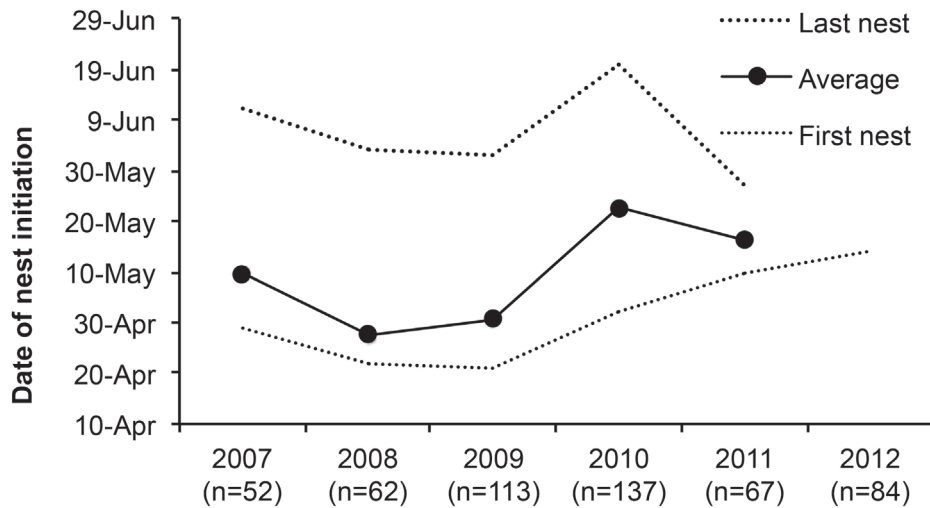


Figure S13. First, average, and last dates for nests initiated by Common murre at Castle Rock National Wildlife Refuge, Del Norte County, CA. The date of nest initiation was defined as the day that an egg was laid at a nest-site, which was accurate to ± 3.5 days. The sample size (n) represents the total number of nests observed per year.

Pelagic Fishes off Southern California Current System

Data and Analysis The spring 2012 Coastal Pelagic Species (CPS) survey was conducted aboard one NOAA research vessel, *Bell M. Shimada* (April 11–April 30) and a chartered research vessel, the R/V *Ocean Starr* (March 26–April 29). The *Ocean Starr* covered the area off the West Coast of U.S. from Cape Flattery, Washington to Point Conception, California with most of the stations off California located within the area from north of San Francisco to Point Conception (CalCOFI lines 56.3 to 80.0 from April 5 to April 28). The *Shimada* covered the area from San Diego, California (CalCOFI line 93.8) to Monterey Bay (CalCOFI line 68.3). The NOAA ship *Shimada* also occupied the primary CalCOFI lines, 76.7 to 93.3, from March 23 to April 7 for the spring CalCOFI cruise. During the DEPM and CalCOFI surveys, PairoVET tows, bongo tows, and CUFES were conducted aboard both vessels while surface trawls were conducted only during the spring CPS survey. Data from spring CPS surveys on both ships were included in the estimation of spawning biomass of Pacific sardines.

Ichthyoplankton data from all spring cruises were used to examine the spatial distributions of Pacific sardine, northern anchovy, and jack mackerel.

SEABIRDS AND MAMMALS

Breeding Success and Diets of Seabirds at Yaquina Head

Data and Analysis Reproductive success represents the proportion of breeding pairs that successfully fledged young as calculated by the mean among 10 to 12 plots

each containing 7 to 25 breeding pairs that were monitored every 1 to 3 days. Murre chicks that remained on the colony ≥ 15 days were considered successfully reared to fledging age. Diet data were collected on 2 to 5 days per week during the chick-rearing period. Single prey items carried in the bill of adult murre were digitally photographed for identification.

Breeding Success and Diets of Seabirds at Castle Rock

Data and Analysis To monitor breeding seabirds at Castle Rock National Wildlife Refuge (hereafter Castle Rock), a remotely-controlled camera monitoring system was installed at the colony in 2006. During the breeding season of 2012, the camera monitoring system failed on 22 June prior to the completion of nesting efforts. As a result, many breeding parameters that were previously quantified for the seabirds at Castle Rock could not be determined during the 2012 breeding season, including nesting success and diet. However, we were able to determine the timing of nest initiation for common murre; in 2012, the first nest was initiated on 15 May, between 4 and 32 days later than all other years of study (fig. S13). Although the average nest initiation date could not be determined due to uncertainties resulting from equipment failure, we concluded that nesting began later than usual in 2012.

At-sea Density of Seabirds off Southern California

Data and Analysis Counts of marine birds at sea have been conducted in conjunction with seasonal CalCOFI/CCE-LTER cruises since May 1987 (Veit et al. 1996). The resulting database now contains 90 surveys

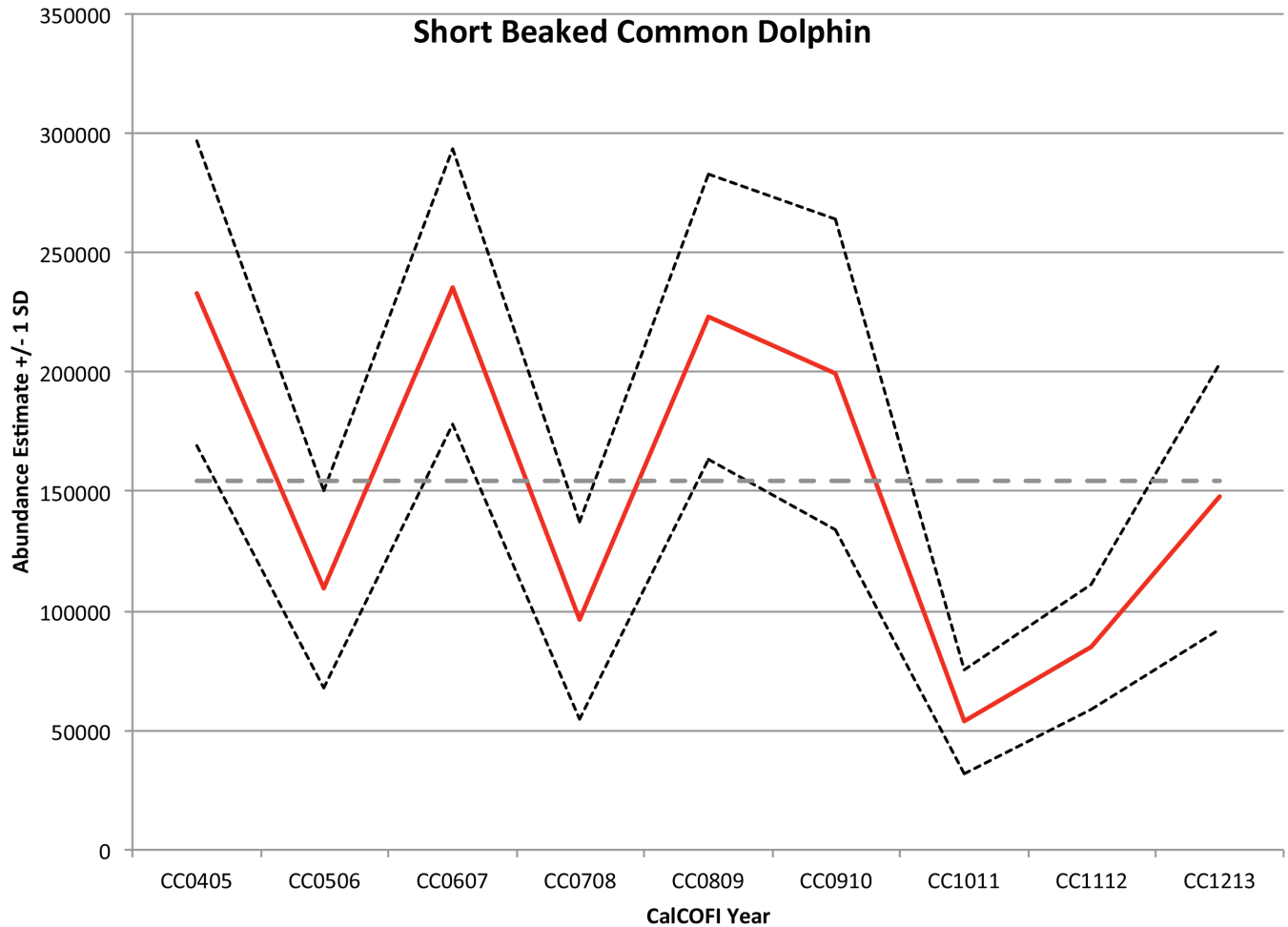


Figure S14. Estimated abundance of short-beaked common dolphins by CalCOFI year from summer 2004–spring 2013. Black dashed lines represent +/- 1 SD. Horizontal grey line represents global abundance across all years/surveys.

over 26 years, including information on seabird distribution and abundance through August 2012. Here, we illustrate patterns of variability in the relative abundance of two species, the sooty shearwater (*Puffinus griseus*) and Cassin’s auklet (*Ptychoramphus aleuticus*) expressed as natural log of density ($\ln [\text{birds km}^{-2} + 1]$). Both species prey upon euphausiid crustaceans, ichthyoplankton, and small pelagic fish and squid.

Productivity and Condition of Sea Lions at San Miguel Island

Data and Analysis San Miguel Island, California (34.03°N, 120.4°W) is one of the largest colonies of California sea lions, representing about 45% of the U. S. breeding population. As such, it is a useful colony to measure trends and population responses to changes in the marine environment.

We used the number of pups alive at the time of the live pup census conducted in late July and the average weights of pups at 4 months and 7 months of age

between 1997 and 2012 as indices of the population response to annual conditions in the CCS.

The number of live pups in late July represents the number of pups that survived from birth to about 6 weeks of age. Live pups were counted after all pups were born (between 20–30 July) each year. A mean of the number of live pups was calculated from the total number of live pups counted by each observer.

Each year, between 200 and 500 pups were weighed when about 4 months old. Pups were sexed, weighed, tagged, branded, and released. Up to 60 pups were captured in February and weighed and measured at 7 months of age. Of the 60 pups captured in February, up to 30 pups were branded and provided a longitudinal data set for estimating a daily growth rate between 4 months and 7 months old.

We used a linear mixed-effects model fit by REML in R to predict average weights on 1 October and 1 February in each year because the weighing dates were not the same among years. The model contained random effects

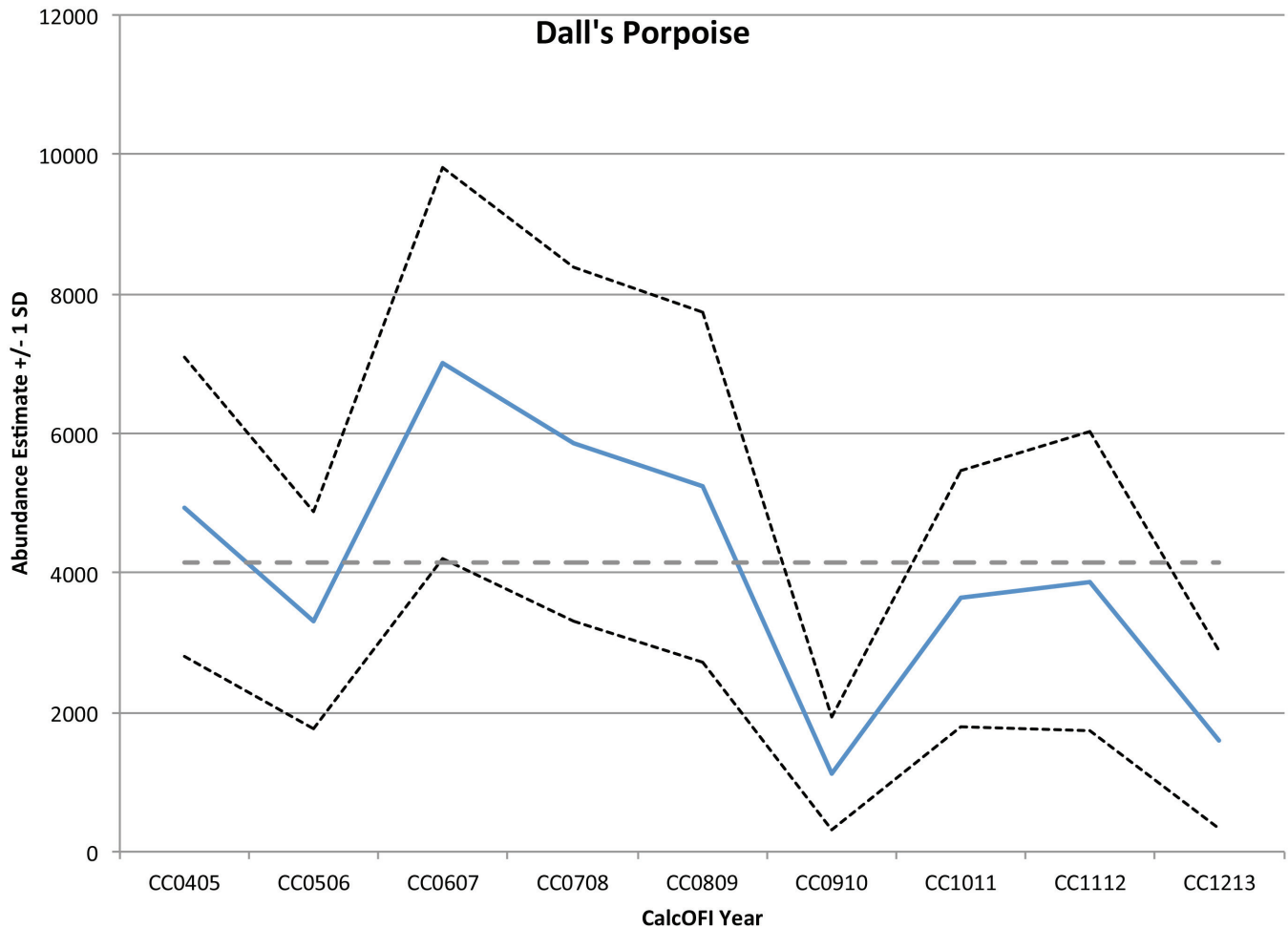


Figure S15: Estimated abundance of Dall's porpoise by CalCOFI year from summer 2004–spring 2013. Black dashed lines represent ± 1 SD. Horizontal grey line represents global abundance across all years/surveys.

with a sex and days interaction (days = the number of days between weighing and 1 October or 1 February), which allowed the growth rate to vary by sex and year, and a full interaction fixed effects of sex and days. The average weights between 1997 and 2012 were compared to the long-term average for the average pup weights between 1975 and 2012.

Comment on Unusual Mortality Event (UME)

At this time (July 2013), the cause of the UME is unknown. The similarities in the population response to the 2013 UME and to the 1997–98 El Niño are striking. However, environmental indices of mean sea surface temperature anomalies and upwelling strength during the 2012–13 in central California did not indicate abnormal oceanographic patterns (e.g., positive sea surface temperature anomalies greater than 1°C, strongly negative upwelling patterns) that are normally associated with a change in sea lion prey availability and lower pup weights. Instead, the period was characterized by anom-

alously strong upwelling and cool sea surface temperatures, which usually produce good foraging conditions for females and robust pups. Estimates of prey availability and abundance from the spring and summer CalCOFI cruises and other fisheries stock assessments and satellite telemetry and food habits studies of lactating females are ongoing and will address whether prey abundance or availability was reduced during the period of the UME. The results from pups sampled for diseases at the stranding centers and pups and lactating females at the rookeries are not yet available.

Cetacean Density and Abundance on the Southern CalCOFI Lines

Short-beaked common dolphins and Dall's porpoise are two of the most frequently encountered small cetaceans in the southern CalCOFI study area with overall abundances of ~154,000 (CV = 16.3) and ~4,100 (CV = 20.1), respectively. Short-beaked common dolphins typically occur in warm-temperate waters $\geq 16^\circ\text{C}$

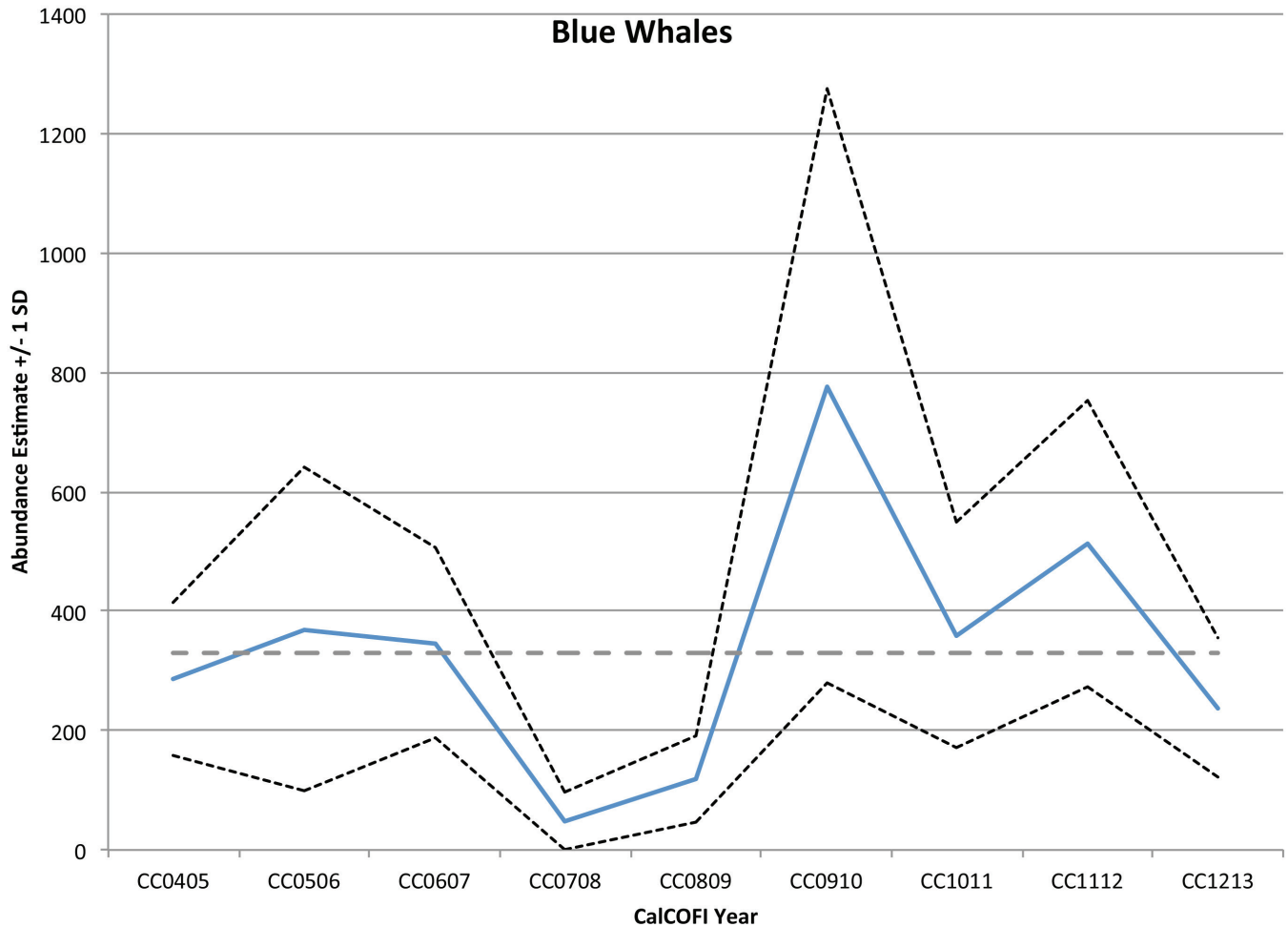


Figure S16. Estimated abundance of blue whales by CalCOFI year from summer 2004–spring 2013. Black dashed lines represent ± 1 SD. Horizontal grey line represents global abundance across all years/surveys.

(Becker et al. 2010), and are distributed in southern and central California across all four seasons. Dall’s porpoise are usually encountered in cooler, upwelling-modified water $<17^{\circ}\text{C}$ (Forney et al. 2012) and are more frequently sighted during the cooler water periods of winter and spring (Becker et al. 2010). Both species have distributions that extend well outside the southern CalCOFI study area, with annual differences in the extent of movement into southern California waters. The annual variations in density and abundance observed for these two species since 2004 coincides with observed annual variations in water temperature; increased abundance of common dolphins was observed during the warmer water years in 2004/2005, 2006, and 2009/2010, whereas Dall’s porpoise exhibited increased abundance during the colder water years of 2007/2008, 2010/2011, 2011/2012 (figs. S14 and S15). During the 2012/2013 sampling period, common dolphins exhibited increased abundance while Dall’s porpoise showed decreases in abundance, supporting the annual variable

patterns of abundance observed since the study began in 2004.

Blue whales and fin whales were two of the most frequently encountered baleen whale species with overall abundances of ~ 330 ($\text{CV} = 27.9$) and ~ 765 ($\text{CV} = 20.9$) respectively. The foraging distributions of baleen whales, off California vary depending on where and when their prey are concentrated, which is largely determined by marine ecosystem features and dynamic climatic and oceanic processes (Munger et al. 2009).

Annual variations in blue whale abundance generally agree with observed annual variations in the biomass of their primary prey item, *Euphausia pacifica* (Ohman, unpublished data) (fig. S16). Low blue whale abundance in 2008/2009 corresponded with the lowest *Euphausia pacifica* mean biomass values recorded since 2004; peak abundance values for blue whales in 2009/2010 corresponded the highest *Euphausia pacifica* mean biomass values reported between 2004–10. Despite low abundance of blue whales in 2007/2008, zooplankton biomass off

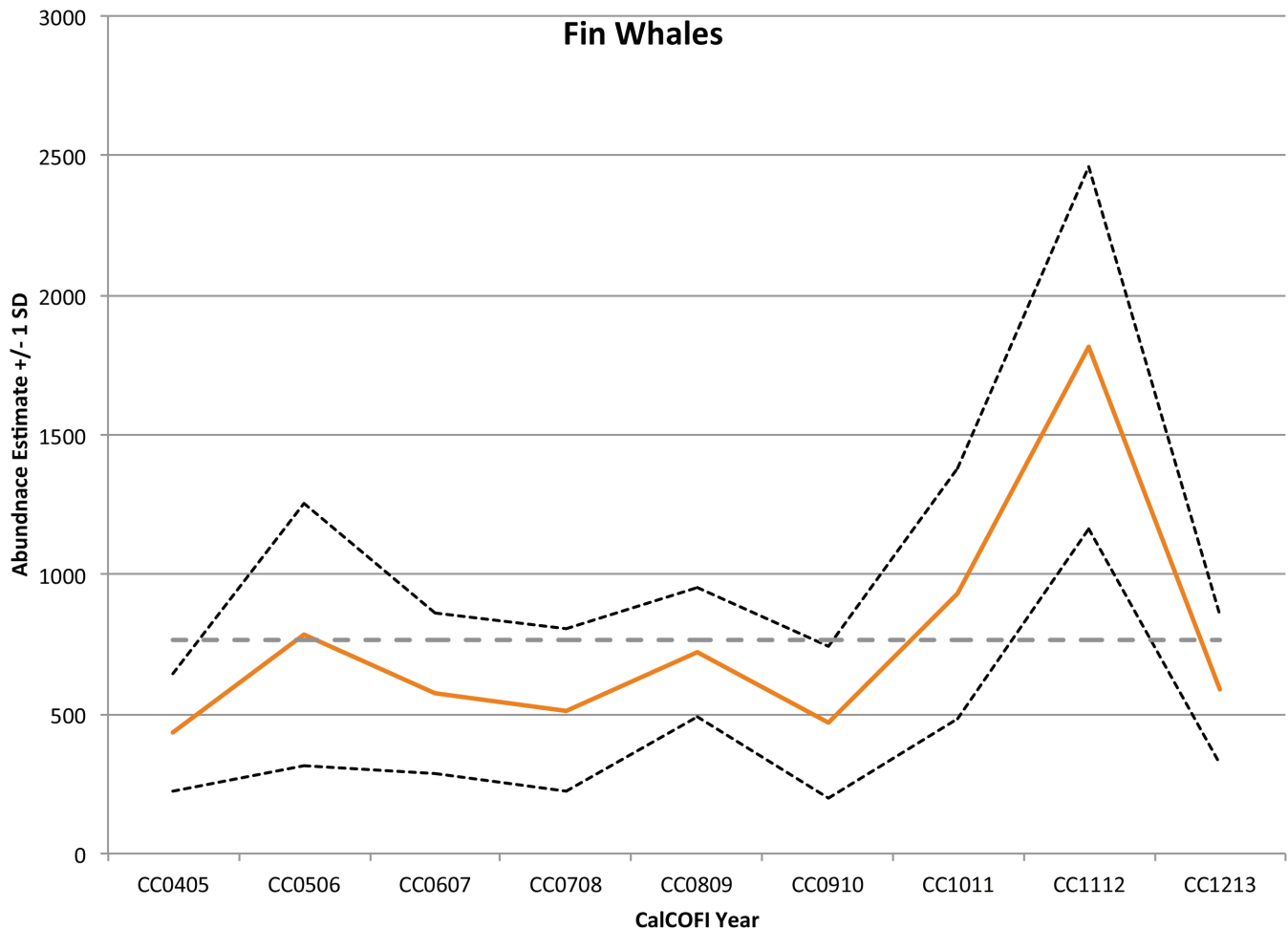


Figure S17. Estimated abundance of fin whales by CalCOFI year from summer 2004–spring 2013. Black dashed lines represent ± 1 SD. Horizontal grey line represents global abundance across all years/surveys.

southern California was relatively high, suggesting that blue whales may have been utilizing prey resources outside of the southern CalCOFI study area, likely off central California, where the largest positive anomaly in euphausiid abundance occurred over the past 20 years (Bjorkstedt et al. 2012). In 2012/2013, blue whale abundance decreased suggesting lower zooplankton biomass in the region; however, zooplankton data for 2012/2013 is not yet available for comparison.

Annual variations in fin whale abundance observed from 2004–13 were less pronounced than those observed for blue whales with the exception of the 2011/2012 season (fig. S17); relatively consistent abundance estimates across years may be a function of the wider range of prey items, including krill and small schooling fishes, consumed by fin whales, allowing for opportunistic feeding in a variety of regions off southern California despite pronounced annual fluctuations in zooplankton biomass. The 2011/2012 fin whale abundance estimates were more than twice the global value, which corresponds

with the second highest mean zooplankton displacement volume for spring since 2004 as well as higher than average values for sardine eggs in spring 2012. In 2012/2013, estimated fin whale abundance estimates decreased to near the global estimate, suggesting lower prey biomass in the region; however, zooplankton data for 2012/2013 is not yet available for comparison.

LITERATURE CITED

- Auth, T. D. 2011. Analysis of the Spring–Fall Epipelagic Ichthyoplankton Community in the Northern California Current in 2004–09 and Its Relation to Environmental Factors. California Cooperative Oceanic Fisheries Investigations Reports 52:148–167.
- Becker, E.A., K.A. Forney, M. C. Ferguson, D. G. Foley, R. C. Smith, J. Barlow, and J. V. Redfern. 2010. Comparing California Current cetacean–habitat models developed using in situ and remotely sensed sea surface temperature data. Marine Ecology Progress Series 413:163–183.
- Bjorkstedt, E., R. Goericke, S. McClatchie, E. Weber, W. Watson, N. Lo, B. Peterson, B. Emmett, R. Brodeur, J. Peterson, M. Litz, J. Gomez-Valdez, G. Gaxiola-Castro, B. Lavaniegos, F. Chavez, C. A. Collins, J. Field, K. Sakuma, P. Warzybok, R. Bradley, J. Jahncke, S. Bograd, F. Schwing, G. S. Campbell, J. Hildebrand, W. Sydeman, S. Thompson, J. Largier, C. Halle, S.Y. Kim, and J. Abell. 2012. State of the California Current 2010–2011:

- Regional Variable Responses to a Strong (But Fleeting?) La Niña. California Cooperative Oceanic Fisheries Investigations Report 52:36–68.
- Bjorkstedt, E. P., R. Goericke, S. McClatchie, E. Weber, W. Watson, N. Lo, B. Peterson, B. Emmett, R. Brodeur, J. Peterson, M. Litz, J. Gomez-Valdez, G. Gaxiola-Castro, B. Lavaniegos, F. Chavez, C. A. Collins, J. Field, K. Sakuma, P. Warzybok, R. Bradley, J. Jahncke, S. Bograd, F. Schwing, G. S. Campbell, J. Hildebrand, W. Sydeman, S. A. Thompson, J. L. Largier, C. Halle, S. Y. Kim, and J. Abell. 2011. State of the California Current 2010–11: Regionally Variable Responses to a Strong (but Fleeting?) La Niña. California Cooperative Oceanic Fisheries Investigations Reports 52:36–68.
- Bjorkstedt, E. P., R. Goericke, S. McClatchie, E. Weber, W. Watson, N. Lo, B. Peterson, B. Emmett, J. Peterson, R. Durazo, G. Gaxiola-Castro, F. Chavez, J. T. Pennington, C. A. Collins, J. Field, S. Ralston, K. Sakuma, S. J. Bograd, F. B. Schwing, Y. Xue, W. J. Sydeman, S. A. Thompson, J. A. Santora, J. Largier, C. Halle, S. Morgan, S. Y. Kim, K. P. B. Merckens, J. A. Hildebrand, and L. M. Munger. 2010. State of the California Current 2009–10: Regional Variation Persists through Transition from La Niña to El Niño (and Back?). California Cooperative Oceanic Fisheries Investigations Reports 51:39–69.
- Daly, E. A., T. D. Auth, R. D. Brodeur, and W. T. Peterson. 2013. Winter ichthyoplankton biomass as a predictor of early summer prey fields and survival of juvenile salmon in the northern California Current. *Marine Ecology Progress Series* 484:203–217.
- Forney, K. A., M. C. Ferguson, E. A. Becker, P. C. Fiedler, J. V. Redfern, J. Barlow, I. L. Vilchis, and L. T. Ballance. 2012. Habitat-based spatial models of cetacean density in the eastern Pacific Ocean. *Endangered Species Research* 16:113–133.
- García-Cordova, J. M. Robles, and J. Gomex-Valdes. 2005. Informe de datos de CTD. Campaña 0504/05. B/O Francisco de Ulloa. 14 Abril–5 Mayo de 2005. Informe Técnico. Departamento de Oceanografía Física, CICESE 119 pp.
- García-Reyes, M. and J. L. Largier. 2012. Seasonality of coastal upwelling off central and northern California: New insights, including temporal and spatial variability. *Journal of Geophysical Research-Oceans* 117:doi:10.1029/2011jc007629.
- Holm-Hansen, O., C. J. Lorenzen, R. W. Holmes, and J. D. H. Strickland. 1965. Fluorometric Determination of Chlorophyll. *Journal du Conseil* 30:3–15.
- Kaplan, D. M., C. Halle, J. Paduan, and J. L. Largier. 2009. Surface currents during anomalous upwelling seasons off central California. *Journal of Geophysical Research-Oceans* 114:doi:10.1029/2009jc005382.
- Kim, S. Y., E. J. Terrill, and B. D. Cornuelle. 2008. Mapping surface currents from HF radar radial velocity measurements using optimal interpolation. *Journal of Geophysical Research-Oceans* 113.
- Largier, J. L., B. A. Magnell, and C. D. Winant. 1993. Subtidal Circulation over the Northern California Shelf. *Journal of Geophysical Research-Oceans* 98:18147–18179.
- Munger, L. M., D. Camacho, A. Havron, G. Campbell, J. Calambokidis, A. Douglas, and J. Hildebrand. 2009. Baleen Whale Distribution Relative to Surface Temperature and Zooplankton Abundance Off Southern California, 2004–08. California Cooperative Oceanic Fisheries Investigations Reports 50:155–168.
- Phillips, A. J., R. D. Brodeur, and A. V. Sunstov. 2009. Micronekton community structure in the epipelagic zone of the northern California Current upwelling system. *Progress in Oceanography* 80:74–92.
- Sakuma, K. M., S. Ralston, and V. G. Weststad. 2006. Interannual and spatial variation in the distribution of young-of-the-year rockfish (*Sebastes* spp.): expanding and coordinating a survey sampling frame. California Cooperative Oceanic Fisheries Investigations Reports 47:127–139.
- Smith, R. L., A. Huyer, and J. Fleischbein. 2001. The coastal ocean off Oregon, from 1961 to 2000: is there evidence of climate change or only of Los Niños? *Progress in Oceanography* 49:63–93.
- Terrill, E. J., M. Otero, L. Hazard, D. Conlee, J. Harlan, J. Kohut, P. Reuter, T. Cook, T. Harris, and K. Lindquist. 2006. Data Management and Real-time Distribution in the HF-Radar National Network. OCEANS 2006, IEEE, 10.1109/OCEANS.2006.306883.
- Veit, R. R., P. Pyle, and J. A. McGowan. 1996. Ocean warming and long-term change in pelagic bird abundance within the California current system. *Marine Ecology Progress Series* 139:11–18.
- Venrick, E. and T. L. Hayward. 1984. Determining chlorophyll on the 1984 CalCOFI surveys. California Cooperative Oceanic Fisheries Investigations Reports 25:74–79.
- Yentsch, C. S. and D. W. Menzel. 1963. A Method for the Determination of Phytoplankton Chlorophyll and Phaeophytin by Fluorescence. *Deep-Sea Research* 10:221–231.